

PROCEEDINGS OF SPIE

[SPIDigitalLibrary.org/conference-proceedings-of-spie](https://spiedigitallibrary.org/conference-proceedings-of-spie)

Nano-tomography of dental composites with wide color matching

Mattia Humbel, Mario Scheel, Christine Tanner, Griffin Rodgers, Georg Schulz, et al.

Mattia Humbel, Mario Scheel, Christine Tanner, Griffin Rodgers, Georg Schulz, Corinne Carlucci, Jeannette von Jackowski, Guido Sigron, Andrés Izquierdo, Timm Weitkamp, Bert Müller, "Nano-tomography of dental composites with wide color matching," Proc. SPIE 12242, Developments in X-Ray Tomography XIV, 122420Q (14 October 2022); doi: 10.1117/12.2635928

SPIE.

Event: SPIE Optical Engineering + Applications, 2022, San Diego, California, United States

Nano-tomography of dental composites with wide color matching

Mattia Humbel^a, Mario Scheel^b, Christine Tanner^a, Griffin Rodgers^a, Georg Schulz^a, Corinne Carlucci^a, Jeannette von Jackowski^a, Guido Sigron^a, Andrés Izquierdo^a, Timm Weitkamp^b, and Bert Müller^a

^aBiomaterials Science Center, Department of Biomedical Engineering, University of Basel, Gewerbestrasse 14, 4123 Allschwil, Switzerland

^bSynchrotron SOLEIL, L'Orme des Merisiers, 91190 Saint-Aubin, France

ABSTRACT

Dental restorations should match the color of the surrounding enamel. Carefully selecting the appropriate shade for the filling material is a challenge for dentists. Moreover, tooth color can change over time due to habits such as smoking or drinking coffee. In the last few years, single-shade dental composites have come to the market. They rely on a chameleon effect to provide acceptable to good color matching regardless of the tooth color. The chameleon effect refers to a dental filling's ability to guide light in such a way that its color blends in with that of the tooth. Structural color is a contributing factor to the chameleon effect and an active area of research where structures at the submicron scale play a critical role. We investigated the size, shape, and three-dimensional spatial arrangement of filler particles in single-shade dental resin composites. Cylindrical samples of dental composites were prepared and imaged with the transmission X-ray microscope at the ANATOMIX beamline, Synchrotron SOLEIL, France. The centers of the filler particles were determined from the tomography data. Combined with shape information from scanning electron microscopy, a Monte Carlo approach was used to model the transmittance for light at wavelengths from the visible to the ultraviolet. The results were compared to optical transmission measurements. The combination of nanotomography and simulation can thus help to understand the influence of the size and distribution of filler particles on the chameleon effect.

Keywords: dental filling, composite shades, structural color, chameleon effect, synchrotron radiation-based tomography, transmission X-ray microscopy

1. INTRODUCTION

Dental resin composites, consisting of ceramic filler particles embedded in a polymer matrix, are in widespread use for dental restorations.¹ Conventionally, the composites are coloured with pigments and are available in a limited set of shades. Dentists need to stock filling material in several colors and for each restoration determine the best-fitting shade, while also considering that wetness can change the appearance of the material. Additionally, tooth color may change over time due to aging and habits such as smoking or drinking coffee, tea, or red wine, leading to unsatisfying results.

The chameleon effect, or blending effect, partially compensates for color mismatch between restoration and tooth. A blending of the colors close to the material interface has been demonstrated.^{2,3} Over the last few years, several single-shade resin composites have emerged that come in only one shade and rely on the chameleon effect to produce a color consistent with the enamel surrounding the restoration. They include Tokuyama Dental's Omnichroma,⁴ Kulzer's Venus Pearl One,⁵ and R-dental's Chroma Fill.⁶ Other products, such as 3M Oral Care's Filtek Universal,⁷ come in a reduced set of shades and rely on the chameleon effect to cover the whole range of tooth colors.

The Omnichroma dental composite in particular was shown to exhibit structural color produced by the uniform-sized 260 nm diameter silica-zirconia spheres that constitute the filler.⁸ The structural color arising from disordered arrays of core-shell particles, similar to the ones constituting the Omnichroma filler, has been modeled using Monte Carlo simulations of multiple scattering by Hwang *et al.*⁹

M.H.: mattia.humbel@unibas.ch

2. MATERIALS AND METHODS

Three single-shade and one multi-shade (Filtek Universal) universal dental resin composites were procured: Omnichroma PLT (Tokuyama Dental, Tokyo, Japan), Venus Pearl ONE PLT (Kulzer, Hanau, Germany), ArtOral Chroma FILL (R-dental, Hamburg, Germany), Filtek Universal XW (3M, St. Paul, USA). Cylindrical samples with a target diameter of 100 μm and a length of around 10 mm were fabricated by rolling the material out to the desired shape, followed by ultraviolet light curing with a Bluephase G4 curing light (Ivoclar Vivadent, Schaan, Liechtenstein). For transmission measurements, disks of the Omnichroma composite with a target thickness of 100 μm and a radius of around 10 mm were fabricated by pressing portions of the material between blocks of acrylic glass.

Samples were placed in the full-field transmission X-ray microscope using Zernike phase contrast at the ANATOMIX beamline, Synchrotron SOLEIL, France.^{10–12} A monochromatic beam with a mean photon energy of 10 keV was used. 500 projections were acquired over 180°, with an exposure time of 500 ms per projection and an isotropic pixel size of 34.7 nm. Each measurement was repeated four times in immediate succession to increase signal-to-noise ratio.

Tomographic reconstruction by filtered back-projection was performed using the `tomopy` framework (version 1.11.0).¹³ This is not the standard reconstruction pipeline at the ANATOMIX beamline. A Paganin filter¹⁴ with characteristic length 200 nm was applied to the projections to reduce noise. Sample motion during a scan was estimated by two-dimensional rigid registration between corresponding projections of subsequent scans, using the `elastix` toolbox (version 5.0).^{15,16} The projections were shifted accordingly and averaged projections from all four scans were then reconstructed.

For the Omnichroma tomography dataset, a $45 \times 200 \times 200$ pixel subvolume was selected, where the spherical filler particles were segmented by applying a Jerman blob enhancement filter¹⁷ at length scale $\sigma = 65$ nm and sensitivity $\tau = 0.75$, thresholding at a “blobness” value of 0.01 and extracting the centers of labelled regions with `scikit-image`.¹⁸

As a second measurement the optical transmittance of a disk of Omnichroma dental composite was determined for wavelengths between 190 and 2500 nm at 5 nm intervals, using a Lambda 1500+ spectrophotometer (PerkinElmer, Waltham, USA) with integrating sphere.

The optical transmittance of a composite disk was modeled by a Monte Carlo simulation of multiple scattering, using the `structcol` package.^{9,19} A single run for one set of parameters and one wavelength consisted of 10 000 trajectories and 500 scattering events per trajectory. This was repeated for 50 evenly spaced wavelengths between 250 and 800 nm. The composite was assumed to consist of filler particles with a spherical ZrO_2 core of radius r_c and a spherical SiO_2 shell of outer radius $r = 130$ nm, occupying a volume fraction ρ surrounded by a homogeneous polymer matrix of refractive index n_m . A sample of thickness d in air was considered. The wavelength-dependent refractive index for ZrO_2 and SiO_2 was interpolated from data by Filmetrics²⁰ and Philipp,²¹ respectively. Absorption was assumed to be homogeneous across the whole sample, and equal to the one determined for SiO_2 by Khashan.²² Simulations were run for a range of values for the sample thickness d , core radius r_c/r , refractive index of the polymer matrix n_m , and volume fraction ρ .

3. RESULTS

Nanotomography showed substantial differences in the mesoscopic structure between the four dental composites, see Fig. 1. For Omnichroma, Fig. 1a, the filler particles are spherical and of roughly equal size. The Filtek Universal composite, Fig. 1b, consists of irregularly shaped filler particles with diameters ranging from a few hundred nanometers to several micrometers. It also features smaller, highly attenuating components. The filler particles of the Venus Pearl One composite, Fig. 1c, are of polyhedral shape, while for ArtOral Chroma Fill, Fig. 1d, no internal structures could be resolved with our setup.

The quality of the tomographic images could be substantially improved by combining four scans acquired in immediate succession. They were individually reconstructed, aligned with three-dimensional rigid registration, and then averaged. Fig 2a shows a virtual slice through a single dataset, and Fig 2b the same slice in the averaged dataset. To account for sample motion over the course of a single tomographic acquisition, the displacement

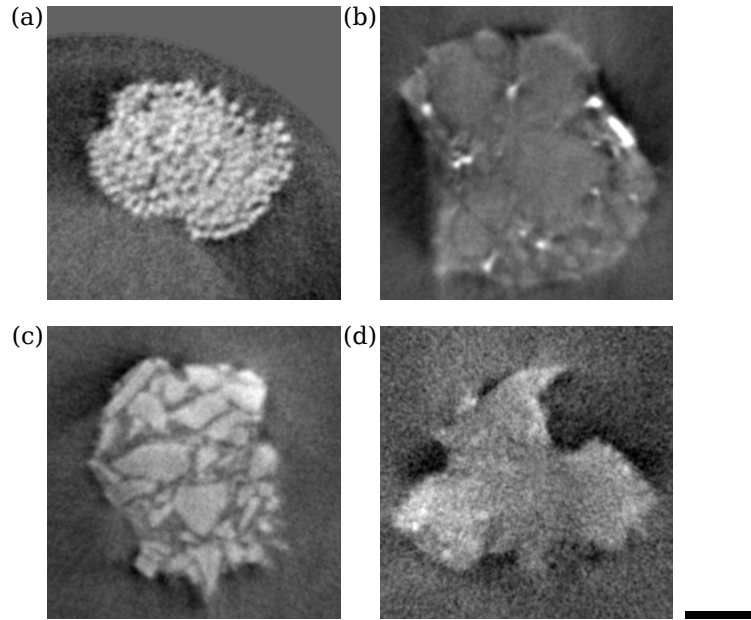


Figure 1. Virtual slices through tomograms of four single-shade dental composites. (a) Omnichroma, (b) Filtek Universal, (c) Venus Pearl One, and (d) Chroma Fill. The scale bar is 2 μm .

between corresponding projections in the four datasets was determined by two-dimensional rigid reconstruction. The vertical displacements are shown in Fig. 2d. By correcting for this motion, the quality could be further improved, as can be seen in Fig. 2c.

For the Omnichroma samples, ellipsoid-like aggregations of filler particles were observed, with tight packing of spheres at the domain border and a lower filler density inside, see Humbel *et al.*, Fig. 5.²³ The domains were a few micrometers in size. The spheres centers that were determined for a subvolume of the Omnichroma nanotomography dataset had a mean distance to the nearest neighbor of (256 ± 2) nm, leading to the conclusion that the spheres are just touching each other. A three-dimensional rendering of perfect spheres at the determined positions is shown in Fig. 3. The region shown is situated at the tip of the cylindrical sample.

A spectrophotometric measurement of the optical transmittance of a disk of Omnichroma, represented by grey dots in Fig. 4, showed that the material is mostly transparent in the visible and near-infrared range, with a transmittance between 74.9 and 91.7%. For ultraviolet light a large drop in transmittance was observed, from 74.9% at 400 nm to 3.1% at 350 nm. A small peak could be observed centered at 264 nm, with a full width at half maximum of 20 nm.

The spectral transmittance computed from a Monte Carlo simulation was consistent with experiment for a sample thickness $d = 50 \mu\text{m}$, volume fraction $\rho = 0.7$, core radius $r_c/r = 0.3$, and refractive index of the polymer matrix $n_m = 1.67$. Fig. 4 shows the change of the transmittance when varying the core radius and the refractive index of the polymer matrix. The core radius strongly impacts the behavior, as can be seen from the reduced transmittance between 400 and 650 nm for $r_c/r = 0.4$. The refractive index of the polymer matrix was observed to govern the slope of the main step (between 300 and 400 nm). A larger refractive index resulted in a steeper rise of the transmittance.

4. DISCUSSION

With nanotomography, the differences in structure between the four dental resin composites on the sub-micrometer scale were made visible. Significant differences in the optical properties have been shown previously for Omnichroma, Venus Pearl One, and Filtek Universal.²⁴ The strength of the chameleon effect, quantified by the color adjustment potential, has been examined for the Omnichroma and Filtek Universal composites, showing

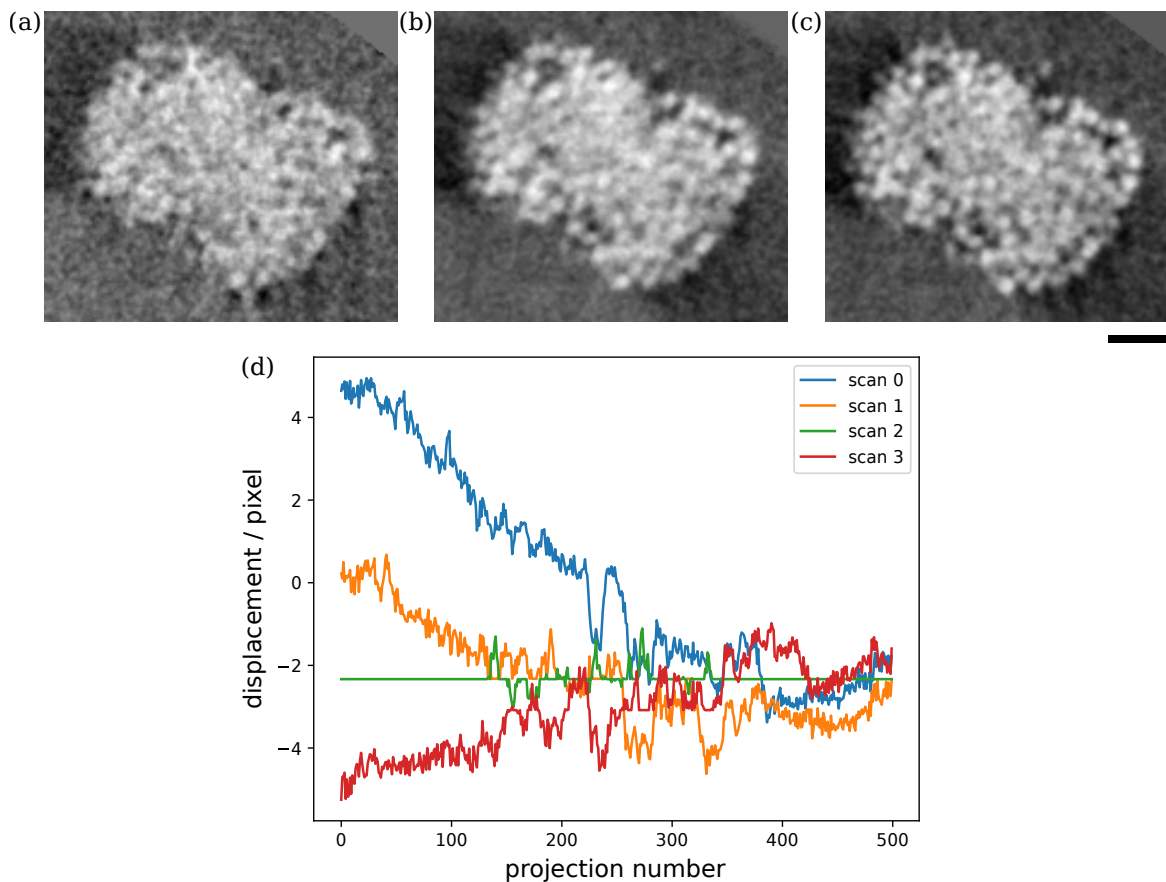


Figure 2. Virtual slices through reconstructed data showing the tip of a sample consisting of the Omnichroma dental composite. (a) Reconstruction from a single 180° scan. (b) Average of four individually reconstructed scans, aligned in image space by three-dimensional rigid registration. (c) Averaged reconstruction from a motion-corrected set of projections. (d) Vertical displacements applied to individual projections in order to correct for sample motion. The scale bar is $1\ \mu\text{m}$.

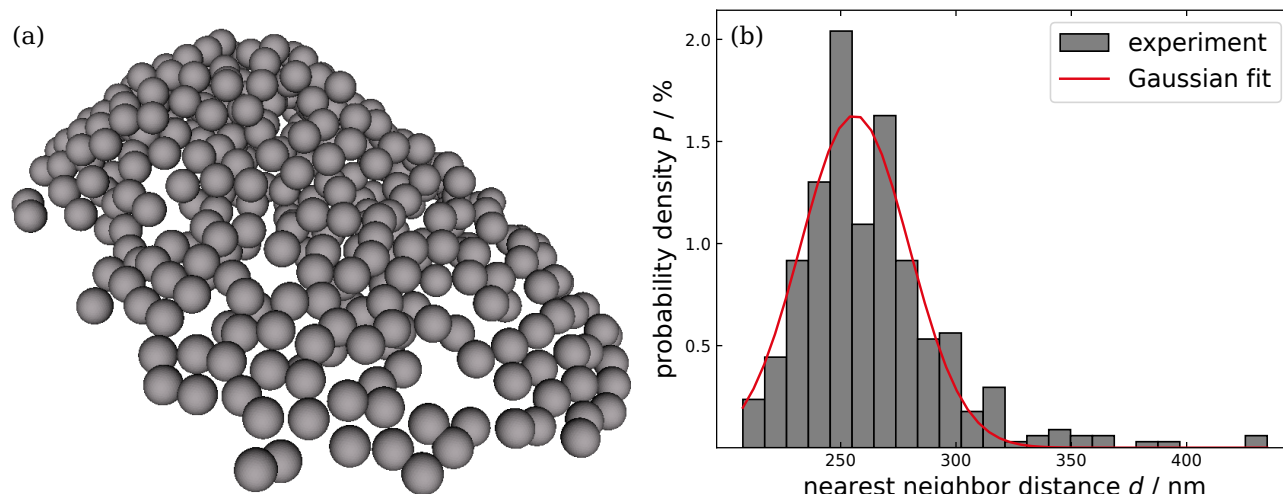


Figure 3. (a) Volume rendering of spheres with diameter $260\ \text{nm}$ at the positions derived from segmentation of nanotomography data from a selected Omnichroma specimen. (b) Histogram of the distance to the nearest neighbour for the segmented sphere centers.

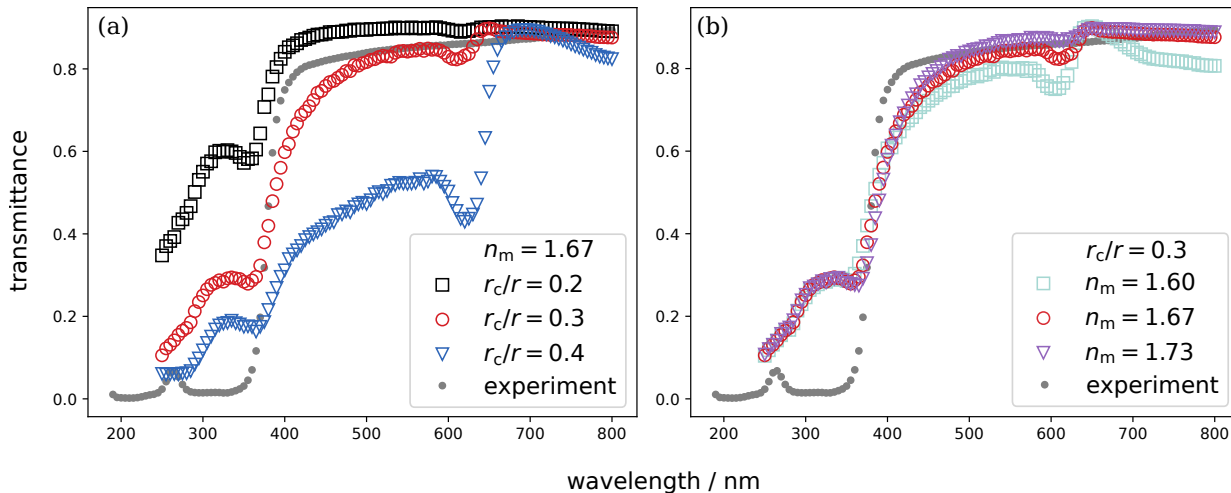


Figure 4. Optical transmittance of a slab of dental composite determined by Monte Carlo simulation, compared to the spectrophotometric measurement (grey dots). (a) Simulation with the refractive index of the polymer matrix n_m equal to 1.67 and comparing three values for the radius of the filler core r_c/r (as a fraction of the particle radius r). (b) Simulation with the core radius r_c/r equal to 0.3 and comparing three values for the matrix refractive index n_m . The assumed volume fraction ρ was 0.7 and the sample thickness d was 50 μm in both settings.

better color adjustment for Omnicroma.²⁵ The optical properties as well as the color adjustment potential are expected to depend not only on the chemical composition of filler and matrix, but also on the mentioned sub-micrometer structure.

In the Omnicroma sample, inhomogeneities in the distribution of filler particles were revealed, specifically micrometer-sized ellipsoid-like domains with tight packing along the border and a lower particle density inside the domain compared to outside. Angle-independent structural color results from positive interference of light scattered off nanostructures with no long-ranged order, and resonance is therefore determined by the mean spacing between neighboring sites.¹⁹ Thus the presence of domains with larger or smaller average spacing is expected to influence the optical properties of the whole restoration.

The mean distance between neighboring sphere centers determined for the Omnicroma composite, 256 nm, is consistent with the filler particle diameter indicated by the manufacturer as 260 nm⁴ and confirmed with small-angle X-ray scattering.²³

Magkiriadou *et al.* have used a single-scattering model to calculate the reflection from colloidal glasses of 170, 240, and 330 nm PMMA particles, where they were able to qualitatively predict the reflection, including the position of peaks due to structural color.¹⁹ Hwang *et al.* modeled polystyrene nanoparticles with radii of 94, 109, and 138 nm using a Monte Carlo simulation for multiple scattering and could quantitatively predict the reflectance.⁹ The same Monte Carlo multi scattering approach was applied here for the Omnicroma composite. By testing a range of values for the parameters that were unknown *a priori*, a configuration was found that is in reasonable agreement with the transmission measurement. This approach, however, did not yet address the observed inhomogeneous distribution of filler particles.

5. CONCLUSION

We have demonstrated how tomographic imaging using a transmission X-ray microscope using Zernike phase contrast can be employed to investigate the mesoscopic structure of dental resin composites relevant for the chameleon effect. For the Omnicroma composite, we combined this knowledge with a Monte Carlo simulation to show the dependence of the spectral transmittance on the composition, structure and arrangement of spherical filler particles. A similar approach can be extended to other composites, although the irregular filler shapes will be an additional challenge. The available data can be used in more sophisticated simulations, for instance taking also into account the inhomogeneous distribution of filler particles.

ACKNOWLEDGMENTS

We thank Robert Lominski and Ivo Stemmler from PerkinElmer, and Robert Sterchi from ZHAW for providing access to the spectrophotometer. ANATOMIX is an Equipment of Excellence (EQUIPEX) funded by the *Investments for the Future* program of the French National Research Agency (ANR), project *NanoimagesX*, grant no. ANR-11-EQPX-0031.

REFERENCES

- [1] Cho, K., Rajan, G., Farrar, P., Prentice, L., and Prusty, B. G., “Dental resin composites: A review on materials to product realizations,” *Composites Part B: Engineering* **230**, 109495 (2022).
- [2] Paravina, R. D., Westland, S., Imai, F. H., Kimura, M., and Powers, J. M., “Evaluation of blending effect of composites related to restoration size,” *Dental Materials* **22**(4), 299–307 (2006).
- [3] Tsubone, M., Nakajima, M., Hosaka, K., Foxton, R. M., and Tagami, J., “Color shifting at the border of resin composite restorations in human tooth cavity,” *Dental Materials* **28**(8), 811–817 (2012).
- [4] Tokuyama Dental, “Omnichroma,” tech. rep. (2019).
- [5] Kulzer, “Venus diamond / pearl One shade.” https://www.kulzerus.com/en_us/en_us/dentist_2/products_from_a_to_z_1/venus_16/venus_diamond_pearl_one.aspx. Accessed: 15 August 2022.
- [6] R-dental, “ArtOral chroma fill product information,” tech. rep. (2021).
- [7] 3M Oral Care, “3M Filtek universal restorative,” tech. rep. (2019).
- [8] Kobayashi, S., Nakajima, M., Furusawa, K., Tichy, A., Hosaka, K., and Tagami, J., “Color adjustment potential of single-shade resin composite to various-shade human teeth: Effect of structural color phenomenon,” *Dental Materials Journal* **40**(4), 1033–1040 (2021).
- [9] Hwang, V., Stephenson, A. B., Barkley, S., Brandt, S., Xiao, M., Aizenberg, J., and Manoharan, V. N., “Designing angle-independent structural colors using Monte Carlo simulations of multiple scattering,” *Proceedings of the National Academy of Sciences* **118**(4) (2021).
- [10] Weitkamp, T., Scheel, M., Giorgetta, J. L., Joyet, V., Roux, V. L., Cauchon, G., Moreno, T., Polack, F., Thompson, A., and Samama, J. P., “The tomography beamline ANATOMIX at synchrotron SOLEIL,” *Journal of Physics: Conference Series* **849**, 012037 (June 2017).
- [11] Weitkamp, T., Scheel, M., Perrin, J., Daniel, G., King, A., Roux, L., V., Giorgetta, J. L., Carcy, A., Langlois, F., Desjardins, K., Meneglier, C., Cerato, M., Engblom, C., Cauchon, G., Moreno, T., Rivard, C., Gohon, Y., and Polack, F., “Microtomography on the ANATOMIX beamline at Synchrotron SOLEIL,” in [*Proceedings of the 14th International Conference on Synchrotron Radiation Instrumentation*], (2022). Accepted.
- [12] Scheel, M., Perrin, J., Koch, F., Daniel, G., Giorgetta, J.-L., Cauchon, G., King, A., Yurgens, V., Roux, V. L., David, C., and Weitkamp, T., “Current status of hard X-ray nano-tomography on the transmission microscope at the ANATOMIX beamline,” in [*Proceedings of the 14th International Conference on Synchrotron Radiation Instrumentation*], (2022). Accepted.
- [13] Gürsoy, D., De Carlo, F., Xiao, X., and Jacobsen, C., “TomoPy: a framework for the analysis of synchrotron tomographic data,” *Journal of Synchrotron Radiation* **21**, 1188–1193 (Sep 2014).
- [14] Paganin, D., Mayo, S. C., Gureyev, T. E., Miller, P. R., and Wilkins, S. W., “Simultaneous phase and amplitude extraction from a single defocused image of a homogeneous object,” *Journal of Microscopy* **206**(1), 33–40 (2002).
- [15] Klein, S., Staring, M., Murphy, K., Viergever, M. A., and Pluim, J. P. W., “*elastix*: A toolbox for intensity-based medical image registration,” *IEEE Transactions on Medical Imaging* **29**(1), 196–205 (2010).
- [16] Shamonin, D., Bron, E., Lelieveldt, B., Smits, M., Klein, S., and Staring, M., “Fast parallel image registration on cpu and gpu for diagnostic classification of alzheimer’s disease,” *Frontiers in Neuroinformatics* **7** (2014).
- [17] Jerman, T., Pernuš, F., Likar, B., and Špiclin, Ž., “Blob Enhancement and Visualization for Improved Intracranial Aneurysm Detection,” *IEEE Transactions on Visualization and Computer Graphics* **22**, 1705–1717 (June 2016).

- [18] Walt, S. v. d., Schönberger, J. L., Nunez-Iglesias, J., Boulogne, F., Warner, J. D., Yager, N., Gouillart, E., and Yu, T., “scikit-image: image processing in Python,” *PeerJ* **2**, e453 (June 2014).
- [19] Magkiriadou, S., Park, J.-G., Kim, Y.-S., and Manoharan, V. N., “Absence of red structural color in photonic glasses, bird feathers, and certain beetles,” *Phys. Rev. E* **90**, 062302 (Dec 2014).
- [20] Filmetrics, “Refractive index of ZrO₂, zirconium dioxide.” <https://www.filmetrics.com/refractive-index-database/ZrO2/Zirconium-Dioxide>. Accessed: 30 May 2022.
- [21] Philipp, H., “Silicon dioxide (SiO₂) (glass),” in [*Handbook of Optical Constants of Solids*], Palik, E. D., ed., 749–763, Academic Press, Burlington (1997).
- [22] Khashan, M. and Nassif, A., “Dispersion of the optical constants of quartz and polymethyl methacrylate glasses in a wide spectral range: 0.2–3 μm ,” *Optics Communications* **188**(1), 129–139 (2001).
- [23] Humbel, M., Mattle, C., Scheel, M., Diaz, A., Jerjen, I., Lominski, R., Sterchi, R., Schulz, G., Izquierdo, A., Sigron, G., Deyhle, H., and Müller, B., “Dental composites for wide color matching,” in [*Bioinspiration, Biomimetics, and Bioreplication XII*], Martín-Palma, R. J., Knez, M., and Lakhtakia, A., eds., **12041**, 1204102 (2022).
- [24] Lucena, C., Ruiz-López, J., Pulgar, R., Della Bona, A., and Pérez, M. M., “Optical behavior of one-shaded resin-based composites,” *Dental Materials* **37**(5), 840–848 (2021).
- [25] Durand, L. B., Ruiz-López, J., Perez, B. G., Ionescu, A. M., Carrillo-Pérez, F., Ghinea, R., and Pérez, M. M., “Color, lightness, chroma, hue, and translucency adjustment potential of resin composites using ciede2000 color difference formula,” *Journal of Esthetic and Restorative Dentistry* **33**(6), 836–843 (2021).